ISSN 1070-3284, Russian Journal of Coordination Chemistry, 2016, Vol. 42, No. 3, pp. 187–195. © Pleiades Publishing, Ltd., 2016.
Original Russian Text © E.O. Platonova, V.A. Il'ichev, E.V. Baranov, L.N. Bochkarev, 2016, published in Koordinatsionnaya Khimiya, 2016, Vol. 42, No. 3, pp. 164–172.

Cyclometallated Iridium(III) Complex with 2-(Benzo[*b*]thiophen-2-yl)pyridyl and Norbornene-Substituted Pyrazolonate Ligands and Related Electroluminescent Red Light-Emitting Polymers

E. O. Platonova[a], V. A. Il'ichev[a, b], E. V. Baranov[a, b], and L. N. Bochkarev[a, b, *]

[a] *G.A. Razuvaev Institute of Organometallic Chemistry, Russian Academy of Sciences, ul. Tropinina 49, Nizhni Novgorod, 603950 Russia*

[b] *Nizhni Novgorod State University, pr. Gagarina 23, Nizhni Novgorod, 603950 Russia*

**e-mail: lnb@iomc.ras.ru*

Received June 15, 2015

Abstract—New cyclometallated iridium(III) complex, (NBEpz)Ir(Btp)$_2$ (**I**) (NBEpzH is 1-phenyl-3-methyl-4-(5-bicyclo[2.2.1]hept-5-en-2-yl)-5-pyrazolone, and BtpH is 2-(benzo[*b*]thiophen-2-yl)pyridine), is synthesized. The structure of the compound is determined by X-ray diffraction analysis (CIF file CCDC no. 1406737). Copolymers with the carbazole and iridium-containing fragments in the side chains (P1–P3) are prepared from monomer **I** using the ROMP method (ROMP is Ring-Opening Metathesis Polymerization). Their photoluminescence and electroluminescence properties are studied. Copolymers P1–P3 exhibit an intense photoluminescence and electroluminescence of red color. The maximum current efficiency (17.9 cd/A) and power efficiency (9.1 lm/W) are reached using emitter P2.

DOI: 10.1134/S1070328416030076

INTRODUCTION

Investigations on the development of polymer emission materials for organic light diodes (OLED) have actively been performed in the recent decade [1–5]. The application of polymer electroluminophores and the use of solution technologies make it possible to prepare OLED devices with a large area, which is nearly unattainable in the case of low-molecular emitters under the conditions of vacuum deposition. Polymers with chemically bound luminophore metal complexes are especially interesting among various types of polymeric emitters. Metal-containing polymers can generate emission of various colors, depending on the nature of luminescent metal complexes composing the polymer [6–10]. The polymers with the cyclometallated iridium complexes in the main or side chains demonstrate the highest electroluminescence (EL) characteristics [10]. The variation of the ligand environment in the metal-containing fragments makes it possible to purposefully change the emission properties and to obtain polymeric emitters with a specified luminescence color.

In this work, we report the synthesis of a new cyclometallated iridium(III) complex with 2-(benzo[*b*]thiophen-2-yl)pyridyl and norbornene-substituted pyrazolonate ligands and the preparation using the ROMP method of iridium-containing polymers (P1–P3) based on the complex and having an intense photoluminescence (PL) and EL in the red spectral range.

EXPERIMENTAL

All procedures with readily oxidizable and hydrolyzable substances were carried out in vacuo or in argon using the standard Schlenk technique. The solvents used were thoroughly purified and degassed. Iridium(III) chloride $[Ir(Btp)_2(Cl)]_2$ [11], sodium pyrazolonate (NBEpz)Na [12], carbazole-containing monomer 9-(bicyclo[2.2.1]hept-5-en-2-ylmethyl)-9H-carbazole (L) [13], and $(H_2IMes)(3\text{-Br-Py})_2(Cl)_2Ru{=}CHPh$ (Grubbs catalyst of the third generation) [14, 15] were synthesized using known procedures. 4,7-Diphenyl-1,10-phenanthroline (BATH) and tris(8-hydroxyquinolinato)aluminum (Alq_3) (Aldrich) were used without additional purification.

^{1}H and ^{13}C{1H} NMR spectra were recorded on Bruker DPX-200 (^{1}H NMR: 200 MHz, ^{13}C NMR: 50 MHz) and Bruker Avance III-400 (^{1}H NMR: 400 MHz, ^{13}C NMR: 100 MHz) spectrometers. Signal assignment was performed using 2D gradient spectroscopy: proton–proton (GE-COSY) and proton–carbon (GE-HSQC) correlations. Chemical shifts are indicated in ppm relative to tetramethylsilane used as an internal standard.

IR spectra were recorded on an FSM 1201 FT-IR spectrometer. A sample of compound **I** was prepared by pellet pressing with the substance to KBr ratio equal to 1 : 200. Samples of polymers P1–P3 were prepared as thin films between KBr plates.

The molecular weight distribution of the polymers was determined by gel permeation chromatography on a Knauer chromatograph with a Smartline RID 2300 differential refractometer as a detector equipped with a set of two Phenomenex columns (Phenogel sorbent with a pore size of 10^4 and 10^5 Å, THF as an eluent, 2 mL/min, 40°C). The columns were calibrated by 13 polystyrene standards.

The electronic absorption spectra of compound **I** and polymers P1–P3 in a CH_2Cl_2 solution were recorded on a PerkinElmer Lambda 25 spectrometer. Photoluminescence spectra were obtained on a PerkinElmer LS 55 fluorescence spectrometer. The relative quantum yields of compound **I** and P1–P3 were determined at room temperature in degassed CH_2Cl_2 solutions at an excitation wavelength of 360 nm. The quantum yields were calculated relative to Rhodamine B in ethanol ($\Phi f = 0.70$) [16] using a described procedure [17].

Thermogravimetric analysis was carried out with a PerkinElmer PYRIS 6 TGA thermogravimeter in a dry nitrogen flow (flow rate 80 cm^3/min, heating rate 5°C/min).

Electroluminescence spectra, current density–voltage and luminance–voltage characteristics, and the CIE chromaticity coordinates were obtained on model OLED devices without encapsulation using an automated complex conjugated with a computer and including a GW INSTEK PPE-3323 power source, a GW INSTEK GDM-8246 digital multimeter, and an Ocean Optics USB 2000 spectrofluorimeter.

Synthesis of (NBEpz)Ir(Btp)$_2$ (I). A solution of (NBEpz)Na (0.12 g, 0.39 mmol) in DME (10 mL) was added to a solution of $(Ir(Btp)_2Cl)_2$ (0.20 g, 0.15 mmol) in DME (30 mL) under an argon atmosphere. The reaction mixture was refluxed with a reflux condenser for 30 h, cooled to room temperature, and filtered. The solvent was evaporated in vacuo, and the solid residue was dissolved in chloroform (2 mL) and added to hexane (30 mL). The formed precipitate was separated by centrifugation and dried in vacuo at 50°C. The yield of complex **I** as an orange-red finely crystalline substance stable in air was 0.20 g (71%).

IR (KBr; ν, cm^{-1}): 3052 ν, 1240 δ, 1157 δ, 1075 δ, 999 δ, 758 δ, 752 δ , 713 $\delta(C_{Ar}–H)$; 2855 ν, 2930 ν, 2959 ν, 1476 δ, 1375 δ, 1302 δ, 914 $\delta_s(C_{Alk}–H)$; 1601 $\nu_{as}(C\cdots O)$; 1580 $\nu(C=C_{Ar})$; 1532 ν(C=N); 1532 ν, 1453 ν, 1433 ν, 1397 ν(pyrazole ring); 914 $\delta_s(C–C)$; 692 δ, 627 δ, 612 ν(chelate ring); 513 δ, 488 δ(Ir–O).

According to the data of NMR spectroscopy, complex **I** is a mixture of *endo* and *exo* isomers.

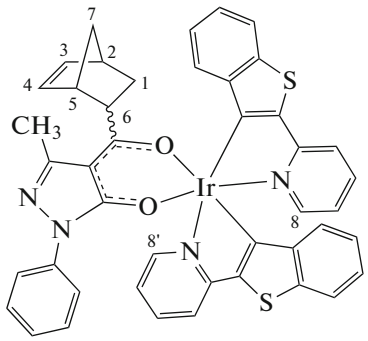

Endo isomer (80%). ^{1}H NMR ($CDCl_3$; δ, ppm): 8.55 (d, J = 5.6 Hz, 0.65H, H^8), 8.44 (d, J = 5.6 Hz, 0.35H, H^8), 8.36 (d, J = 5.6 Hz, 0.35H, $H^{8'}$), 8.16 (d, J = 5.6 Hz, 0.65H, $H^{8'}$), 7.69 (m, 10H, Ar), 7.13 (m, 3H, Ar), 7.00 (dd, J = 9.6, 5.1 Hz, 1H, Ar), 6.94 (m, 2H, Ar), 6.81 (m, 1H, Ar), 6.27 (m, 2H, Ar), 5.60 (dd, J = 5.5, 3.0 Hz, 0.65H, H^3), 5.43 (m, 0.35H, H^3), 5.37 (m, 0.35H, H^4), 4.36 (dd, J = 5.5, 2.8 Hz, 0.65H, H^4), 3.52 (dd, J = 8.5, 4.3 Hz, 0.65H, H^6), 3.30 (m, 0.35H, H^6), 2.92 (s, 0.65H, H^2), 2.89 (s, 0.35H, H^2), 2.71 (s, 0.65H, H^5), 2.61 (s, 0.35H, H^5), 2.53 (s, 1.95H, Me), 2.49 (s, 1.05H, Me), 2.02 (td, J = 10.9, 3.9 Hz, 0.35H, H^1), 1.53 (m, 0.65H, H^1), 1.37 (d, J = 11.3 Hz, 0.65H, $H^{1'}$), 1.24 (t, J = 8.4 Hz, 2H, H^7 and $H^{7'}$), 0.57 (m, 0.35, $H^{1'}$).

Exo isomer (20%). ^{1}H NMR ($CDCl_3$; δ, ppm): 8.51 (d, J = 5.7 Hz, 1H, H^8), 8.31 (t, J = 5.3 Hz, 1H, $H^{8'}$), 7.70 (m, 7H, Ar), 7.60 (m, 1H, Ar), 7.12 (m, 5H, Ar), 6.86 (m, 4H, Ar), 6.33 (t, J = 8.7 Hz, 2H, Ar), 6.09 (br.s, 2H, H^3 and H^4), 2.80 (s, 1H, H^2), 2.88 (dd, J = 8.5, 4.7 Hz, 1H, H^6), 2.67 (s, 1H, H^5), 2.40 (d, J = 5.9 Hz, 3H, Me), 1.94 (d, J = 11.4 Hz, 1H, H^1), 1.21 (m, 2H, H^7 and $H^{7'}$), 1.06 (m, 1H, $H^{1'}$).

All isomers. ^{13}C NMR ($CDCl_3$; δ, ppm): 194.3, 192.2, 165.6, 165.3, 165.1, 163.8, 163.7, 162.0, 161.9, 161.4, 161.32, 161.26, 161.19, 161.15, 159.4, 159.3, 150.0, 149.2, 148.9, 148.8, 148.4, 148.3, 148.2, 148.0, 147.7, 147.6, 139.1, 138.2, 138.1, 138.0, 137.1, 136.1, 135.8, 134.7, 134.1, 130.0, 128.6, 128.4, 124.4, 122.5, 122.3, 122.1, 121.7, 121.6, 119.5, 115.5, 115.4, 115.2, 115.1, 105.9, 105.5, 53.4, 50.0, 49.8, 49.6, 48.1, 47.8, 47.4, 46.7, 46.3, 46.2, 44.9, 43.2, 42.4, 41.9, 41.8, 32.5, 31.4, 29.7, 28.9, 28.3, 18.1, 17.8.

For $C_{44}H_{33}N_4O_2S_2Ir$

anal. calcd., %:	C, 58.32;	H, 3.67.
Found, %:	C, 58.40;	H, 3.75.

Synthesis of copolymer P1. The Grubbs catalyst of the third generation (0.0030 g, 0.0034 mmol) in CH_2Cl_2 (3 mL) was added to a mixture of monomers **I**

(0.0350 g, 0.0386 mmol) and L (0.0845 g, 0.3091 mmol) in CH_2Cl_2 (5 mL). The mixture was stirred at room temperature. The reaction course was monitored by thin layer chromatography. After the end of copolymerization (4 h), several droplets of vinyl ethyl ether was added to the reaction mixture to decompose the catalyst, and the mixture was additionally stirred for 20 min. The formed polymer was precipitated with hexane, additionally purified by reprecipitation with methanol from CH_2Cl_2, and dried in vacuo at room temperature to a constant weight. The yield of copolymer P1 as an orange powder was 0.11 g (92%).

IR (ν, cm^{-1}): 3050 ν, 1534 ν, 1482 δ, 1454 δ, 1377 δ, 1324 δ, 1153 δ, 1062 δ, 1018 δ, 750 δ, 720 δ(C_{Ar}–H); 2923 ν, 2860 ν, 800 δ(C_{Alk}–H); 1604 ν_{as} (C···O); 1579 ν(C=C_{Ar}); 1537 ν (C=N); 1534 ν(pyrazole ring); 1625 ν(C=C); 1261 δ, 1211 δ, 924 δ, 910 δ, 866 δ(C_{Alk}–C); 617 δ(chelate ring); 565 δ, 529 δ(Ir–O). ^{1}H NMR ($CDCl_3$; δ, ppm): 8.01 (m, 36H, Ar), 7.32 (m, 33H, Ar), 7.16 (m, 48H, Ar), 5.28 (m, 18H), 4.04 (m, 16H), 0.6–3.0 (m, 91H).

For $C_{204}H_{185}N_{12}O_2S_2Ir$

anal. calcd., %:	C, 79.22;	H, 6.03.
Found, %:	C, 79.11;	H, 5.97.

M_w = 29900, M_n = 17300, M_w/M_n = 1.7, T_d = 267°C (at 5% mass loss).

Synthesis of copolymer P2 from compounds **I** (0.0250 g, 0.0275 mmol) and L (0.0905 g, 0.3310 mmol) was similar to the procedure described above. The copolymerization time was 4 h. The yield was 0.10 g (88%).

IR (ν, cm^{-1}): 3051 ν, 1535 ν, 1482 δ, 1460 δ, 1380 δ, 1330 δ, 1153 δ, 1065 δ, 1026 δ, 748 δ, 726 δ(C_{Ar}–H); 2943 ν, 2868 ν, 805 δ(C_{Alk}–H); 1601 ν_{as}(C···O); 1581 ν(C=C_{Ar}); 1535 ν(C=N); 1535 ν(pyrazole ring); 1625 ν(C=C); 1264 δ, 1211 δ, 927 δ(C_{Alk}–C); 617 δ(chelate ring); 565 δ, 530 δ(Ir–O).

^{1}H NMR ($CDCl_3$; δ, ppm): 8.02 (m, 36H, Ar), 7.29 (m, 36H, Ar), 7.10 (m, 23H, Ar), 5.15 (m, 20H), 4.12 (m, 15H), 0.6–3.0 (m, 65H).

For $C_{284}H_{261}N_{16}O_2S_2Ir$

anal. calcd., %:	C, 81.48;	H, 6.28.
Found, %:	C, 81.38;	H, 6.23.

M_w = 23300, M_n = 11900, M_w/M_n = 1.9, T_d = 270°C (at 5% mass loss).

Synthesis of copolymer P3 from compounds **I** (0.0200 g, 0.0221 mmol) and L (0.0965 g, 0.3530 mmol) was similar to the procedure described above. The copolymerization time was 4 h. The yield was 0.10 g (86%).

IR (ν, cm^{-1}): 3050 ν, 1534 ν, 1482 δ, 1451 δ, 1380 δ, 1325 δ, 1150 δ, 1065 δ, 1021δ, 750 δ, 726 δ(C_{Ar}–H); 2926 ν, 2865 ν, 800 δ(C_{Alk}–H); 1598 ν_{as}(C···O); 1579 ν(C=C_{Ar}); 1534ν (C=N); 1534 ν(pyrazole ring); 1625 ν(C=C); 1261 δ, 1214 δ, 924 δ(C_{Alk}–C); 615 δ(chelate ring); 566 δ, 529 δ(Ir–O).

^{1}H NMR ($CDCl_3$; δ, ppm): 7.97 (m, 45H, Ar), 7.31 (m, 42H, Ar), 7.13 (m, 62H, Ar), 5.30 (m, 34H), 4.06 (m, 32H), 0.6–3.0 (m, 119H).

For $C_{364}H_{337}N_{20}O_2S_2Ir$

anal. calcd., %:	C, 82.80;	H, 6.43.
Found, %:	C, 82.72;	H, 6.37.

Table1. Crystallographic data and the X-ray diffraction experimental and refinement parameters for complex **I** · 0.25(Me_2CO)

Parameter	Value
Empirical formula	$C_{44.75}H_{34.50}IrN_4O_{2.25}S_2$
FW	920.58
Temperature, K	100(2)
Crystal system	Triclinic
Space group	$P\bar{1}$
a, Å	15.173(1)
b, Å	16.845(1)
c, Å	17.432(1)
α, deg	104.866(1)
β, deg	91.607(1)
γ, deg	115.878(1)
V, Å^3	3823.8(4)
Z	4
F(000)	1832
ρ_{calcd}, g cm^{-3}	1.599
μ, mm^{-1}	3.646
Crystal size, mm	0.34 × 0.31 × 0.10
Scan range θ, deg	1.838–25.999
Ranges of reflection indices	$-18 \leqslant h \leqslant 18$
	$-20 \leqslant k \leqslant 20$
	$-21 \leqslant l \leqslant 21$
Total number of reflections	33473
Number of independent reflections	14908
R_{int}	0.0255
GOOF (F^2)	1.061
R_1, wR_2 ($I > 2\sigma(I)$)	0.0367, 0.0933
R_1, wR_2 (all data)	0.0466, 0.0983
$\Delta\rho_{max}/\Delta\rho_{min}$, *e* Å^{-3}	2.208/–0.751

$M_w = 25600$, $M_n = 16600$, $M_w/M_n = 1.5$, $T_d = 331$°C (at 5% mass loss).

X-ray diffraction analysis. The crystallographic data for compound **I** were collected on a Bruker D8 QUEST automated diffractometer (MoK_α radiation, $\lambda = 0.71073$ Å). The structure was solved by a direct method followed by the refinement using full-matrix least squares for F^2 (SHELXTL) [18]. An absorption correction was applied using the SADABS program [19]. All non-hydrogen atoms were refined in the anisotropic approximation. Hydrogen atoms were placed in the geometrically calculated positions and refined by the riding model. The crystallographic characteristics and the main refinement parameters are presented in Table 1. The crystallographic information for compound **I** was deposited with the Cambridge Crystallographic Data Centre (CIF file CCDC no. 1406737; deposit@ccdc.cam.ac.uk or http://www.ccdc.cam.ac.uk).

Fabrication of OLED devices. A glass plate with the deposited ITO layer (120 nm, 15 Ohm/cm^2) (Lum Tec) acting as an anode served as a support for OLED devices with the configuration ITO/Ir polymer (40 nm)/BATH (30 nm)/Alq_3 (30 nm)/Yb (150 nm). The emission layer of the copolymer was deposited from its solution in CH_2Cl_2 (5 mg/mL) on a Spincoat G3-8 centrifuge (3000 rpm, 30 s) and dried in vacuo at 70°C for 3 h. The layer thickness was determined with a META-900 ellipsometer. A hole-blocking layer of BATH, an electron-transporting layer of Alq_3, and an Yb layer acting as a cathode were deposited by vacuum (10^{-6} mm Hg) evaporation from separated thermoresistant evaporators. The layer thickness was monitored with a calibrated quartz resonator. The active surface area of the devices was a circle with a diameter of 5 mm.

RESULTS AND DISCUSSION

Earlier we synthesized the iridium-containing polymers emitting in the green spectral range from the iridium complex with the phenylpyridyl and norbornene-substituted pyrazolonate ligands [20, 21]. It is known that the cyclometallated iridium complexes with the Btp ligands exhibit the PL and EL of red color [22]. Therefore, norbornene monomer **I** containing the $(Btp)_2Ir$ fragment was synthesized and used for the preparation of iridium-containing polymers luminescing in the red spectral range

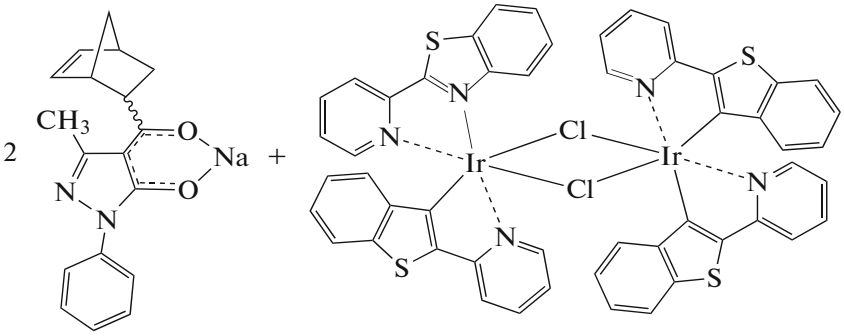

(NBEpz)Na $[Ir(Btp)_2(Cl)]_2$

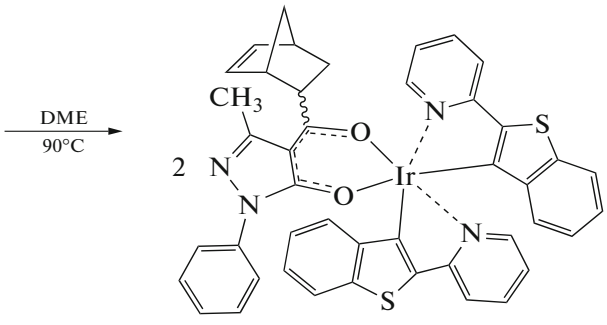

(I)

Complex **I** was synthesized in a high yield as an orange-red finely crystalline substance stable in air, soluble in chloroform, acetone, CH_2Cl_2, and DME, and insoluble in hexane. The NMR method showed

Table 2. Selected bond lengths (Å) and angles (deg) in complex **I**

Bond, Å	Molecule		Angle, deg	Molecule	
	A	B		A	B
Ir(1)–O(1)	2.124(3)	2.149(3)	N(1)Ir(1)N(2)	178.5(1)	178.4(1)
Ir(1)–O(2)	2.137(3)	2.134(3)	O(1)Ir(1)C(7)	175.5(2)	172.1(2)
Ir(1)–N(1)	2.048(4)	2.056(4)	O(2)Ir(1)C(20)	176.1(2)	173.8(2)
Ir(1)–N(2)	2.042(4)	2.044(4)	O(2)Ir(1)C(7)	89.9(2)	90.1(2)
Ir(1)–C(7)	1.981(4)	1.993(5)	C(7)Ir(1)C(20)	91.9(2)	89.5(2)
Ir(1)–C(20)	1.992(4)	2.003(4)	C(20)Ir(1)O(1)	90.0(2)	93.6(1)
O(1)–C(27)	1.257(6)	1.265(5)	O(1)Ir(1)O(2)	88.4(1)	87.7(1)
O(2)–C(29)	1.260(6)	1.264(6)	N(1)Ir(1)O(1)	95.0(1)	92.1(1)
C(19)–C(20)	1.362(6)	1.371(6)	N(1)Ir(1)O(2)	84.2(1)	84.5(1)
N(3)–C(27)	1.366(6)	1.371(5)	N(1)Ir(1)C(7)	80.6(2)	80.1(2)
N(3)–N(4)	1.408(6)	1.396(5)	N(1)Ir(1)C(20)	99.5(2)	101.6(2)
C(27)–C(28)	1.441(7)	1.443(6)	N(2)Ir(1)O(1)	83.4(1)	87.6(1)
C(28)–C(29)	1.423(8)	1.410(7)	N(2)Ir(1)O(2)	95.9(1)	93.9(2)
			N(2)Ir(1)C(7)	100.9(2)	100.1(2)
			N(2)Ir(1)C(20)	80.4(2)	80.1(2)

Table 3. Photophysical characteristics for complex **I** and polymers P1–P3

Compound	λ_{abs}, nm (log ε)	λ_{em}, nm		PL quantum yield, % (CH_2Cl_2)
		film	in CH_2Cl_2	
I	273 (3.60), 331 (3.26), 354 sh (3.15), 450 sh (2.56), 480 (2.64)		614, 659 sh	1.25
P1	263 (4.26), 282 sh (3.95), 288 sh (4.00), 293 (4.12), 317 sh (3.53), 330 (3.64), 345 (3.68), 362 sh (3.13), 455 sh (2.61), 484 (2.69)	621, 658 sh	614, 660 sh	0.65
P2	262 (4.98), 282 sh (4.65), 287 sh (4.70), 293 (4.82), 318 sh (4.21), 330 (4.34), 345 (4.37), 361 sh (3.76), 452 sh (3.11), 482 (3.20)	617, 655 sh	614, 660 sh	0.68
P3	264 (5.40), 283 sh (5.07), 288 sh (5.14), 294 (5.26), 318 sh (4.60), 331 (4.75), 346 (4.81), 362 sh (4.09), 455 sh (3.41), 483 (3.50)	620, 657 sh	614, 660 sh	0.72

that the product was a mixture of *endo* and *exo* isomers in a ratio of 80 : 20.

The X-ray diffraction analysis of complex **I** showed only the *endo* isomer in the single-crystal sample obtained after the crystallization of the compound from acetone. The asymmetric part of the crystal cell contains two molecules of complex **I** (A and B). The crystal cell contains four molecules of complex **I** (two pairs of molecules A and B) and one solvate acetone molecule. Molecules A and B are identical in structure (Table 2). Therefore, when studying the structure of complex **I**, we present the geometric characteristics of molecule A.

In complex **I**, the central iridium atom is coordinated by three bidentate ligands (two Btp and one NBEpz) and has an octahedral coordination (Fig. 1).

The O(1,2) and C(7,20) atoms lie in the base of the octahedron, and the N(1,2) atoms occupy the axial positions.

The N(1)Ir(1)N(2) axial angle is equal to 178.5(1)°, and the Ir–C and Ir–N bond lengths (1.981(4), 1.992(4) and 2.048(4), 2.042(4) Å, respectively) are close to similar distances in the related iridium complexes with the 2-(benzo[*b*]thiophen-2-yl)pyridyl ligands (1.97(2)–2.034(6), 2.043(6)–2.08(2) Å) [23–27]. The Ir(1)–O(1, 2) bond lengths in complex **I** are 2.124(3) and 2.137(3) Å, respectively, and lie in the range of similar distances (2.103(4)–2.14(2) Å) for the iridium complexes with the acetylacetonate and 2-(benzo[*b*]thiophen-2-yl)pyridyl substituents [23–25, 27]. The NBEpz and Btp chelate angles in complex **I** equal to 80.1(2)° and 87.7(1)°, respectively, nearly coincide with similar angles in the related iridium complexes (79.6(2)–81.1(2)° and 88.7(2)–90.3(6)°, respectively) [23–27].

According to the literature data, the inclusion of carbazole groups into polymeric emitters improves their EL characteristics [1]. Therefore, carbazole-containing comonomer L was used for the preparation of the iridium-containing copolymers. The ROMP reactions involving monomers **I** and L occur in the presence of the Grubbs catalyst of the third generation at room temperature and result in the formation of iridium-containing copolymers P1–P3 with different ratios of the organic and metal-containing units

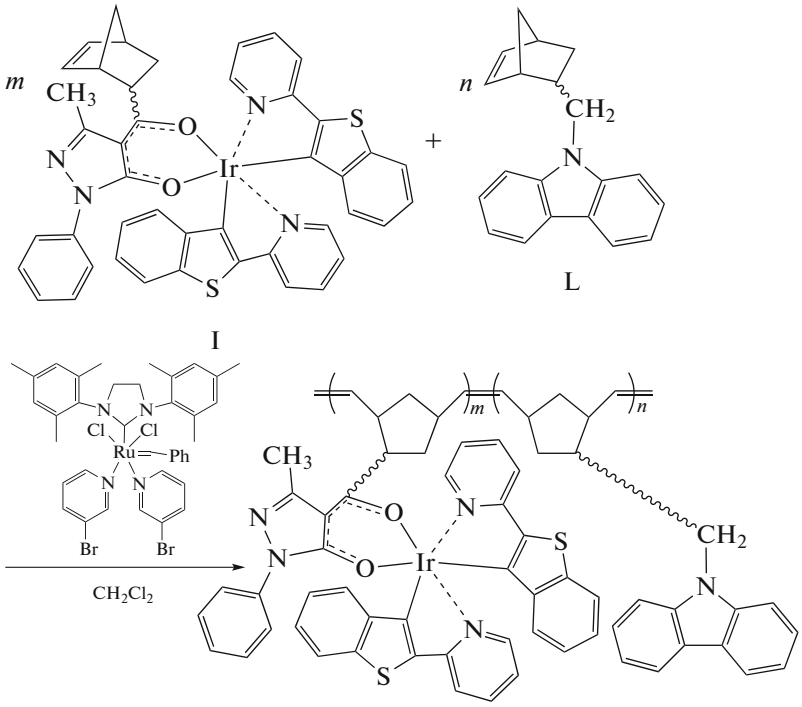

P1 ($m : n = 1 : 8$)
P2 ($m : n = 1 : 12$)
P3 ($m : n = 1 : 16$)

In all reactions, the Grubbs catalyst was used in an amount of 1 mol % with respect to the overall amount of the starting comonomers. It was determined by thin layer chromatography that the copolymerization processes completed within 4 h. Polymer products P1–P3 were isolated as orange powders stable in air and highly soluble in THF, CH_2Cl_2, and $CHCl_3$. The compositions of the copolymers were confirmed by elemental analysis and ^{1}H NMR spectroscopy.

The study of the photophysical properties of the synthesized compounds indicates that the absorption spectrum of complex **I** (Fig. 2, Table 3) is similar to the spectrum of the known iridium(III) acetylacetonate complex $Ir(Btp)_2(Acac)$ [22]. The intense bands with maxima at 273, 331, and 354 nm in the spectrum of complex **I** are attributed to ligand-centered $^1(\pi \rightarrow \pi^*)$ transitions in the 2-(benzo[*b*]thiophen-2-yl)pyridyl and pyrazolonate ligands. The bands with a lower intensity (430–530 nm) can be assigned to metal-to-ligand charge-transfer (MLCT) transitions [22]. The absorption spectra of copolymers P1–P3 contain the bands characteristic of complex **I** and additional intense bands at 260–350 nm due to the $\pi \rightarrow \pi^*$ transitions in the carbazole fragments.

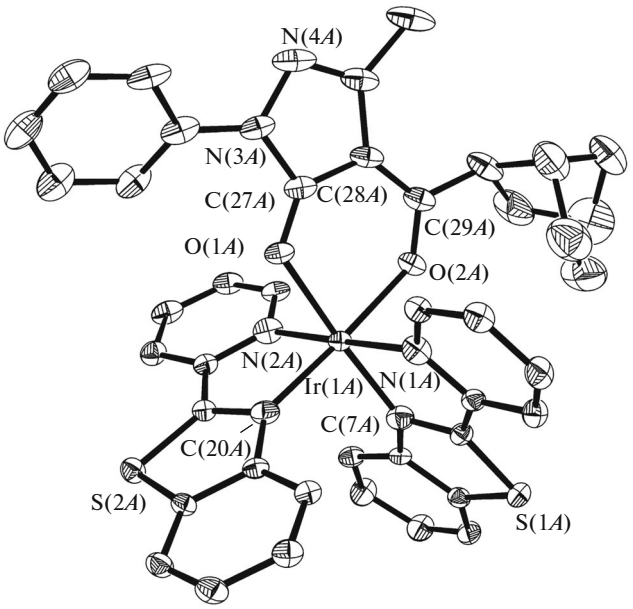

Fig. 1. Structure of molecule A in complex **I** with ellipsoids of 30% probability. Hydrogen atoms are omitted.

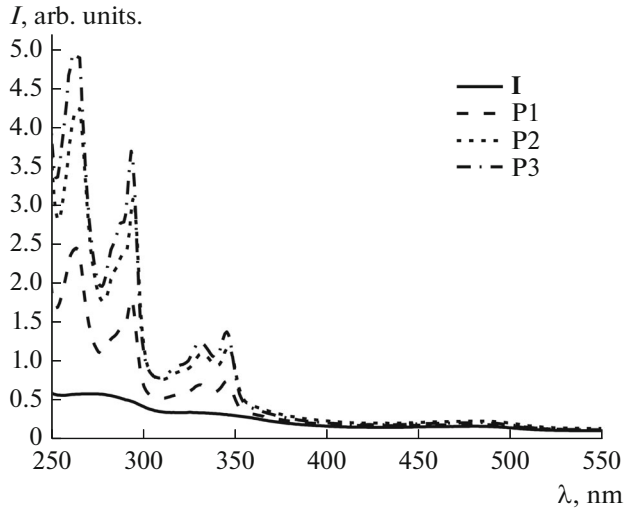

Fig. 2. Absorption spectra of complex **I** and polymers P1–P3 in a CH_2Cl_2 solution.

The PL spectrum of complex **I** (Fig. 3a) in a CH_2Cl_2 solution contains the band with a maximum at 614 nm and the band of a lower intensity at 659 nm (shoulder to the main band), which can be assigned to the ^{3}LC and ^{3}MLCT transitions [22]. Only emission bands attributed to the ^{3}LC and ^{3}MLCT transitions in the iridium-containing fragments appear in the PL spectra of copolymers P1–P3 in solution and in thin films (Fig. 3, Table 3).

The PL quantum yields for copolymers P1–P3 are insignificantly lower than the quantum yield of monomer **I** (Table 3). Probably, this is related to nonradiative losses in the polymer emitters because of the diffusion of triplet excited states along the polymer chain and triplet–triplet annihilation [28, 29].

The EL properties of copolymers P1–P3 were studied for model OLED devices of the configurations ITO/Ir polymer (40 nm)/BATH (30 nm)/Alq_3 (30 nm)/Yb. The EL spectra of the polymer emitters and the working characteristics of the related OLED devices are presented in Figs. 4 and 5 and in Table 4.

The EL spectra of copolymers P1–P3 are similar and contain the bands with maxima at 600–660 nm attributed to the ^{3}LC/^{3}MLCT transitions in the cyclometallated iridium complexes bound to the polymer chain. The absence of the emission from the carbazole groups indicates the efficient transfer of the excitation energy from the polymer matrix to the iridium-containing fragments via the Förster mechanism [30]. The chromaticity coordinates of the OLED devices in the CIE (Commision Internationale de l'Eclairage) diagram (Table 4) correspond to the red color and remain almost unchanged in the whole range of applied volt-

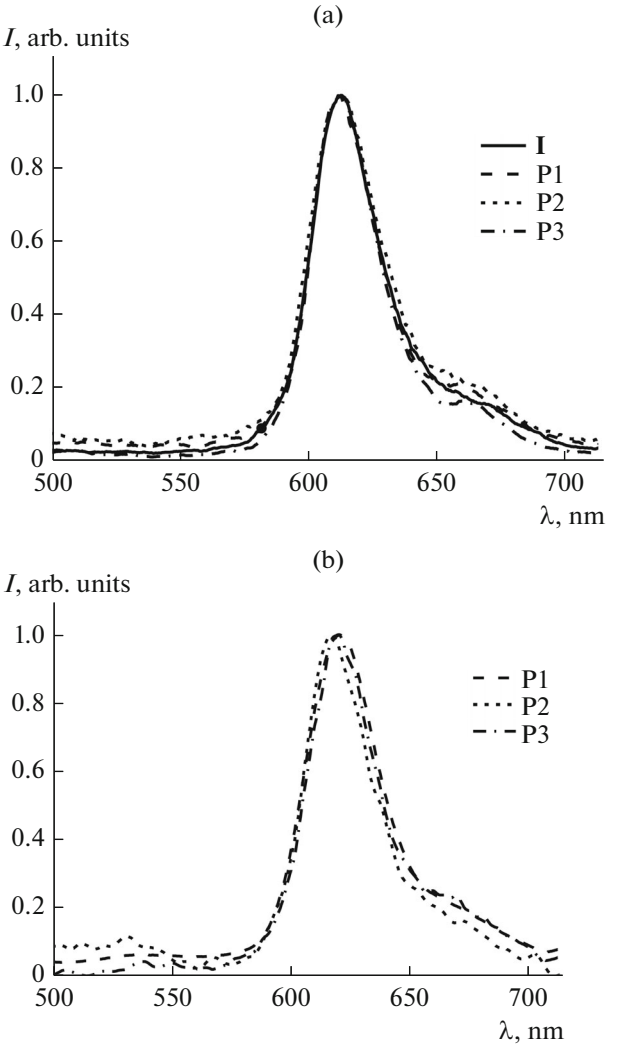

Fig. 3. Normalized PL spectra of (a) complex **I** and polymers P1–P3 in a CH_2Cl_2 solution and (b) polymers P1–P3 in film at room temperature (λ_{exc} = 360 nm).

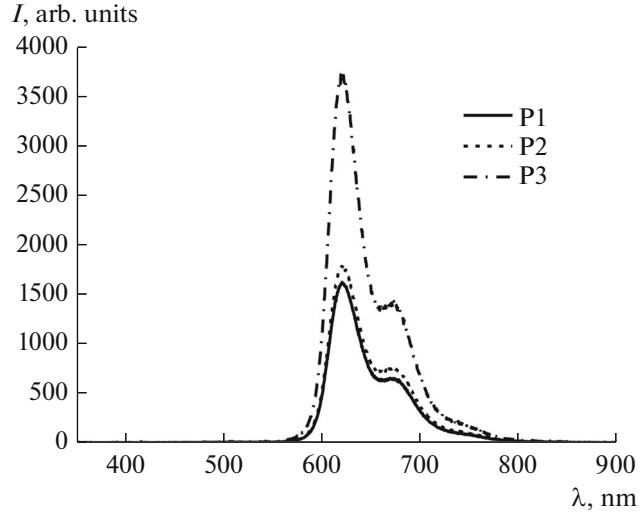

Fig. 4. EL spectra of the OLED devices based on polymers P1–P3 at the maximum luminance.

ages. The highest EL luminance (1116 cd/m^2) was shown by polymer emitter P3. The luminance of the OLED devices based on emitters P1 and P2 is lower (Table 4), but their current and power efficiencies substantially exceed similar characteristics of the OLED based on emitter P3. Note that the maximum current (17.9 cd/A) and power (9.1 lm/W) efficiencies reached for polymer emitter P2 are the highest performance characteristics among the known electroluminescent iridium-containing red-emitting polymers [10, 31, 32].

Thus, new iridium-containing norbornene monomer **I** was synthesized and structurally characterized. Carbon-chain copolymers P1–P3 with the carbazole and iridium-containing fragments in the side chains were obtained from monomer **I** using the ROMP method. The synthesized polymeric emitters exhibit

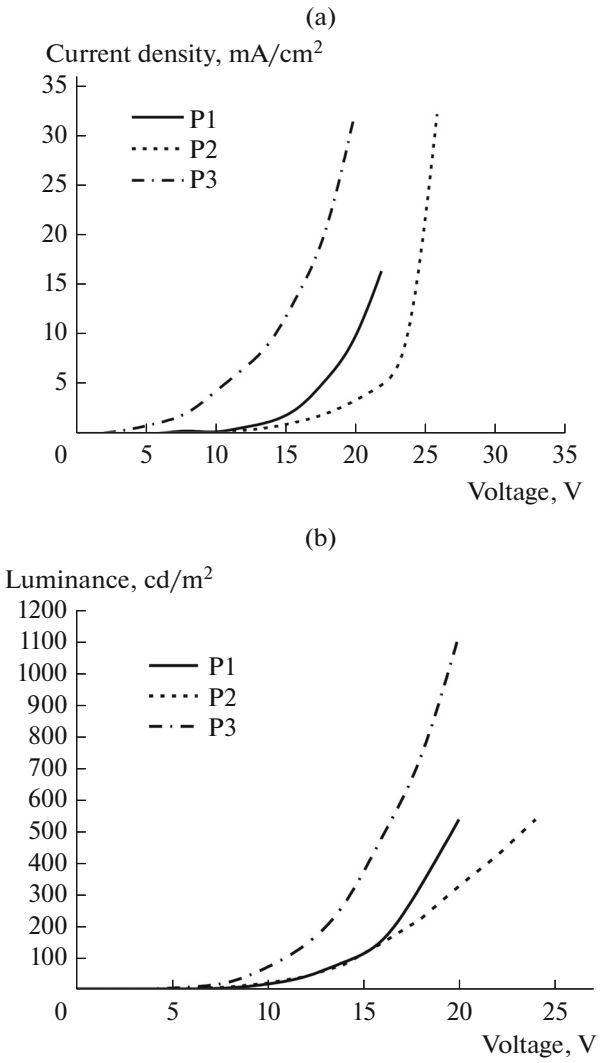

Fig. 5. (a) Current density–voltage and (b) luminance-voltage characteristics of the OLED devices based on polymers P1–P3.

Table 4. Performance characteristics* of the OLED devices based on copolymers P1–P3

Polymer	Turn-on voltage, V**	Maximum luminance, cd/m^2	Maximum current efficiency, cd/A	Maximum power efficiency, lm/W	Chromaticity coordinates in CIE diagram
P1	6.5	535 (20 V)	11.6 (10 V)	3.7 (10 V)	$x = 0.67$ $y = 0.33$
P2	5.5	536 (24 V)	17.9 (8 V)	9.1 (6 V)	$x = 0.67$ $y = 0.33$
P3	5.0	1116 (20 V)	3.6 (18 V)	0.7 (16 V)	$x = 0.67$ $y = 0.33$

* The voltage at which the working characteristics were determined is given in parentheses.
** At the luminance of 1 cd/m^2.

the intense PL and EL of red color. The maximum luminance (1116 cd/m^2) was reached when emitter P3 was used. The highest EL efficiency (17.9 cd/A, 9.1 lm/W) is shown by emitter P2.

ACKNOWLEDGMENTS

This work was supported by the Russian Foundation for Basic Research (project no. 15-43-02178-r_povolzh'e_a) and the Ministry of Education and Science of the Russian Federation (project no. 02.V.49.21.0003).

REFERENCES

1. Grimsdale, A.C., Chan, K.L., Martin, R.E., et al., *Chem. Rev.*, 2009, vol. 109, p. 897.
2. Okamoto, K. and Luscombe, C.K., *Polym. Chem.*, 2011, vol. 2, p. 2424.
3. Guo, X., Baumgarten, M., and Müllen, K., *Prog. Polym. Sci.*, 2013, vol. 38, p. 1832.
4. Zucchi, G., Tondelier, D., Bonnassieux, Y., and Geffroy, B., *Polym. Int.*, 2014, vol. 63, p. 1368.
5. Yang, X., Xu, X., and Zhou, G., *J. Mater. Chem. C*, 2015, vol. 3, p. 913.
6. Bochkarev, L.N., Rozhkov, A.V., and Bochkarev, M.N., *Vysokomol. Soedin.*, 2014, vol. 56, p. 62.
7. Dumur, F., *Org. Electron.*, 2015, vol. 21, p. 27.
8. Bochkarev, L.N., Begantsova, Yu.E., Il'ichev, V.A., and Abakumov, G.A., *Izv. Akad. Nauk, Ser. Khim.*, 2014, p. 2534.
9. Huang, Z., Liu, B., Zhao, J., et al., *RSC Adv.*, 2015, vol. 5, p. 12100.
10. Xu, F., Kim, H.U., Kim, J.-H., et al., *Prog. Polym. Sci.*, 2015, vol. 47, p. 92.
11. Lalevée, J., Dumur, F., Mayer, C.R., et al., *Macromolecules*, 2012, vol. 45, p. 4134.
12. Begantsova, Y.E., Bochkarev, L.N., Malysheva, I.P., et al., *Synth. Met.*, 2011, vol. 161, p. 1043.
13. Liaw, D.-J. and Tsai, C.-H., *Polymer*, 2000, vol. 41, p. 2773.
14. Scholl, M., Ding, S., Lee, C.W., and Grubbs, R.H., *Org. Lett.*, 1999, vol. 1, p. 953.
15. Love, J.A., Morgan, J.P., Trnka, T.M., and Grubbs, R.H., *Angew. Chem., Int. Ed. Engl.*, 2002, vol. 41, p. 4035.
16. López Arbeloa, F., Ruiz Ojeda, P., and López Arbeloa, I., *J. Lumin.*, 1989, Vol. 44, p. 105.
17. Demas, J.N. and Crosby, G.A., *J. Phys. Chem.*, 1971, vol. 75, p. 991.
18. Sheldrick, G.M., *SHELXTL. Version 6.12. Structure Determination Software Suite*, Madison: Bruker AXS, 2000.
19. Sheldrick, G.M., *SADABS. Version 2.01. Bruker/Siemens Area Detector Absorption Correction Program*, Madison: Bruker AXS, 1998.
20. Begantsova, Yu.E., Bochkarev, L.N., Samsonov, M.A., and Fukin, G.K., *Russ. J. Coord. Chem.*, 2013, vol. 39, no. 9, p. 661.
21. Bochkarev, L.N., Begantsova, Yu.E., Platonova, E.O., et al., *Izv. Akad. Nauk, Ser. Khim.*, 2014, no. 4, p. 1001.
22. Lamansky, S., Djurovich, P., Murphy, D., et al., *J. Am. Chem. Soc.*, 2001, vol. 123, p. 4304.
23. Sandee, A.J., Williams, C.K., Evans, N.R., et al., *J. Am. Chem. Soc.*, 2004, vol. 126, p. 7041.
24. Evans, N.R., Devi, L.S., Mak, C.S.K., et al., *J. Am. Chem. Soc.*, 2006, vol. 128, p. 6647.
25. Xu, M.L., Wang, G.Y., Zhou, R., et al., *Inorg. Chim. Acta*, 2007, vol. 360, p. 3149.
26. Rai, V.K., Nishiura, M., Takimoto, M., and Hou, Z., *J. Mater. Chem. C*, 2013, vol. 1, p. 677.
27. Bae, H.J., Chung, J., Kim, H., Park, J., et al., *Inorg. Chem.*, 2014, vol. 53, p. 128.
28. Wilson, J.S., Chawdhury, N., Al-Mandhary, M.R.A., et al., *J. Am. Chem. Soc.*, 2001, vol. 123, p. 9412.
29. Partee, J., Frankevich, E.L., Uhlhorn, B., et al., *Phys. Rev. Lett.*, 1999, vol. 82, p. 3673.
30. Förster, T., *Disc. Faraday Soc.*, 1959, vol. 27, p. 7.
31. Park, J.H., Koh, T.-W., Chung, J., Park, S.H., et al., *Macromolecules*, 2013, vol. 46, p. 674.
32. Zhao, J., Lian, M., Yu, Y., Yan, X., et al., *Macromol. Rapid Commun.*, 2015, vol. 36, p. 71.

Translated by E. Yablonskaya